Forest Ecology and Management 441 (2019) 202–214

Contents lists available at ScienceDirect

Forest Ecology and Management

journal homepage: www.elsevier.com/locate/foreco

Spatial and temporal assessment of responder exposure to snag hazards in post-fire environments

Christopher J. Dunn[a,*], Christopher D. O'Connor[b], Matthew J. Reilly[c], Dave E. Calkin[b], Matthew P. Thompson[b]

[a] College of Forestry, Oregon State University, Corvallis, OR 97331, USA
[b] Rocky Mountain Research Station, US Forest Service, Missoula, MT, USA
[c] Department of Biological Sciences, Humboldt State University, Arcata, CA, USA

ARTICLE INFO

Keywords:
Tree mortality
Snag dynamics
Wildfire risk management
Responder exposure
Salvage logging

ABSTRACT

Researchers and managers increasingly recognize enterprise risk management as critical to addressing contemporary fire management challenges. Quantitative wildfire risk assessments contribute by parsing and mapping potentially contradictory positive and negative fire effects. However, these assessments disregard risks to fire responders because they only address social and ecological resources and assets. In this study, we begin to overcome this deficiency by using a novel modeling approach that integrates remote sensing, field inventories, imputation-based vegetation modeling, and empirical models to quantify post-fire snag hazard in space and time. Snag hazard increased significantly immediately post-fire, with severe or extreme hazard conditions accounting for 47%, 83%, and 91% of areas burned at low, moderate and high-severity fire, respectively. Patch-size of severe or extreme hazard positively correlated with fire size, exceeding > 20,000 ha (60% of our largest fire) 10-years post-fire when reburn becomes more likely. After 10 years, snag hazard declined rapidly as snags fell or fragmented, but severe or extreme hazard persisted for 20, 30 and 35 years in portions of the low, moderate and high-severity fire areas. Because forests are denser and wildfires burn with greater severity than historically, these hazardous conditions may represent novel management challenges where risk of injury or death to responders outweighs the benefits of directly engaging the fire. Mapping snag hazard with our methodology could improve situational awareness for both decision makers and fire responders as they mitigate risk during fire management. However, as more landscapes burn we anticipate increased responder exposure to extremely hazardous conditions, which may further entrench the wildfire paradox as fire managers weigh current response decisions with future challenges. Aligning land management objectives with wildfire management needs, in part by mapping responder exposure to snags and other hazards, could help overcome the wildfire paradox and produce desirable long-term outcomes. This research also demonstrates the importance of interdisciplinary collaboration to account for risk to all aspects of fire prone social-ecological systems as we learn to live with fire in rapidly changing environments.

1. Introduction

Today's wildfire environment is increasingly complex and risky because the unanticipated and unintended consequences of historical forest and fire management (Merschel et al., 2014; Zald and Dunn, 2018), a rapidly changing climate (Jolly et al., 2015; Abatzoglou and Wiliams, 2016), and an expanding wildland urban interface (Haas et al., 2013). Despite these challenges, there is increasing consensus that more of the "right" kind of fire, at the "right" place, and "right" time is necessary to reduce long-term wildfire risk (Moritz et al., 2014; North et al., 2015). Recent fires can reduce the occurrence (Parks et al., 2016), spread (Collins et al., 2009; Parks et al., 2015), and severity (Parks et al., 2014; Larson et al., 2013) of subsequent fires. These fires can also improve the efficiency of suppression operations in some ecosystems (Thompson et al., 2016a, 2016b). However, little information exists regarding the impacts of contemporary fires on responder exposure to future hazards, despite their critical role in realizing wildfire benefits.

Researchers and managers are leveraging technology to create new tools that support wildfire risk management before and during an incident (O'Connor et al., 2016; Dunn et al., 2017b). Quantitative wildfire risk assessments are increasingly integrated into land and fire

* Corresponding author.
E-mail address: chris.dunn@oregonstate.edu (C.J. Dunn).

https://doi.org/10.1016/j.foreco.2019.03.035
Received 29 January 2019; Received in revised form 14 March 2019; Accepted 17 March 2019
Available online 29 March 2019
0378-1127/

management across the western U.S. (Calkin et al., 2010; Scott et al., 2013). One limitation to these risk assessments is their focus on social and ecological resources, forcing incident management teams to assess operational risks during a high pressure and time constrained decision environment (Thompson and Calkin, 2011). Fortunately, there are emerging tools that directly support responder safety (notably focused on exposure to the fire itself) in advance of an incident, including mapping suppression difficulty index (Rodriguez y Silva et al., 2014), potential control locations (O'Connor et al., 2017), escape routes (Campbell et al., 2017), and safety zones (Butler, 2014). Including assessments of risk to fire-responders from the multitude of hazards they encounter would further support response decisions, as well as the development of long-term risk reduction strategies.

Tree death is an important ecological process and one of the most evident consequences of contemporary forest fires (Franklin et al., 1987; Reilly and Spies, 2015). Coarse woody debris functions as a long-term nutrient and carbon store, a primary energy source for saprophyte communities, and a contributor to long-term soil development (Harmon et al., 1986, Tinker and Knight, 2000). Snags and logs are also critical habitat components for a variety of fauna species (Bull et al., 1997; Thomas et al., 1979), especially in dynamic early seral environments (Swanson et al., 2010; Dunn and Bailey, 2012). Despite these positive benefits, hazardous trees and snags remain one of the leading causes of fire responder injury or death (National Interagency Fire Center, 2018), and disturbances creating an abundance of snags exacerbates this potential (Page et al., 2013). Therefore, quantifying snag hazard in post-fire environments, and developing decision support tools (e.g. maps) that account for spatial and temporal variation in this hazard, are important steps towards balancing ecological needs with safe and effective wildfire response.

In this study, we quantify snag hazard for 50 years across recently burned landscapes as part of our broader effort to address responder exposure to hazards. We employ a novel modeling approach that integrates remote-sensing, field inventories, imputation based vegetation modeling, and recently developed statistical models of tree mortality and snag dynamics to combine emerging ecological knowledge with risk management science. Our objective is to quantify snag hazard following fire disturbance in both space and time, and describe the anticipated impacts that elevated snag hazards may have on wildfire management strategies and tactics when these landscapes burn again.

2. Methods

Quantifying and mapping post-fire snag hazard is a multi-step process integrating several datasets and empirical models. Fig. 1 provides a visualization of the sequence of methods described detail in the following paragraphs. Spatially explicit pre-fire tree lists provide the basis for estimating the abundance, size and species of trees that may become snags. A tree mortality model, derived from correlations between individual tree characteristics and the relative differenced Normalized Burn Ratio (RdNBR) (Miller and Thode, 2007), estimates fire effects to create post-fire snag lists. Subsequently, we use a snag dynamics model (snag fall and fragmentation) to capture change across space and time. Lastly, we apply a hazard rating to the snag conditions across the entire spatial and temporal datasets to simplify and rank them in accordance with potential impacts to fire responders.

2.1. Study area

This study focused on fires that primarily burned ponderosa pine (*Pinus ponderosa* subsp. *ponderosa)* and dry-mixed conifer forests along the eastern slopes of the Cascade Mountains in Oregon, USA (Fig. 2). Warm dry summers and cold winters characterize the climate, with precipitation falling mostly as snow. Ponderosa pine was the dominant disturbance-mediated overstory species at lower elevations with increasing abundance of shade-tolerant species at higher elevations. Euro-

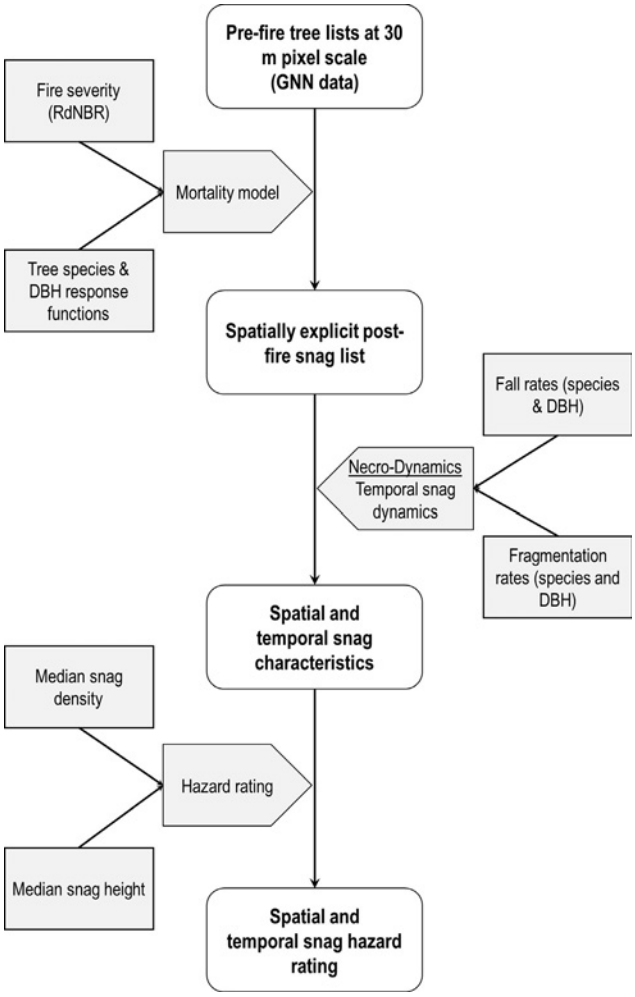

Fig. 1. Flowchart depicting the multi-step process for assessing spatial and temporal snag hazard in post-fire environments. Open shapes represent spatial data layers and shaded shapes are modeling sub-routines.

American colonization altered fire regimes and instituted management practices that increased the abundance of shade-tolerant grand or white fir (*Abies grandis* var. *idahoensis* and *Abies concolor* var. *lowiana*) and Douglas-fir (*Pseudotsuga menziesii* var. *glauca*) across both forest types beginning in the late 19th Century (Merschel et al., 2014; Johnston, 2017; Johnston et al., 2018). Douglas-fir, western larch (*Larix occidentalis* Nutt.), lodgepole pine (*Pinus contorta* subsp. *murrayana*) and incense-cedar (*Calocedrus decurrens* Torr.) are more common in dry-mixed conifer stands with Douglas-fir and grand fir increasing in dominance at upper elevations. We focused on six fires to capture a diversity of fire size and burn severity patterns: 2002 Eyerly, 2002 Cache Mountain, 2003 B&B Complex, 2003 Davis Lake, 2006 Black Crater, and 2007 GW fires (Table 1).

2.2. Spatially explicit tree and snag data

We used predictive maps of pre-fire species composition and forest structure created using the gradient nearest neighbor (GNN) method (Ohmann and Gregory 2002). Maps were obtained from the LEMMA group at Oregon State University and the Pacific Northwest Research Station (https://lemma.forestry.oregonstate.edu/). GNN is a predictive nearest neighbor imputation method that uses field inventory data to develop relationships between vegetation structure, multiple spectral indices (e.g. brightness, greenness, wetness), and gridded data on topography and climate. The LEMMA group used this process to produce

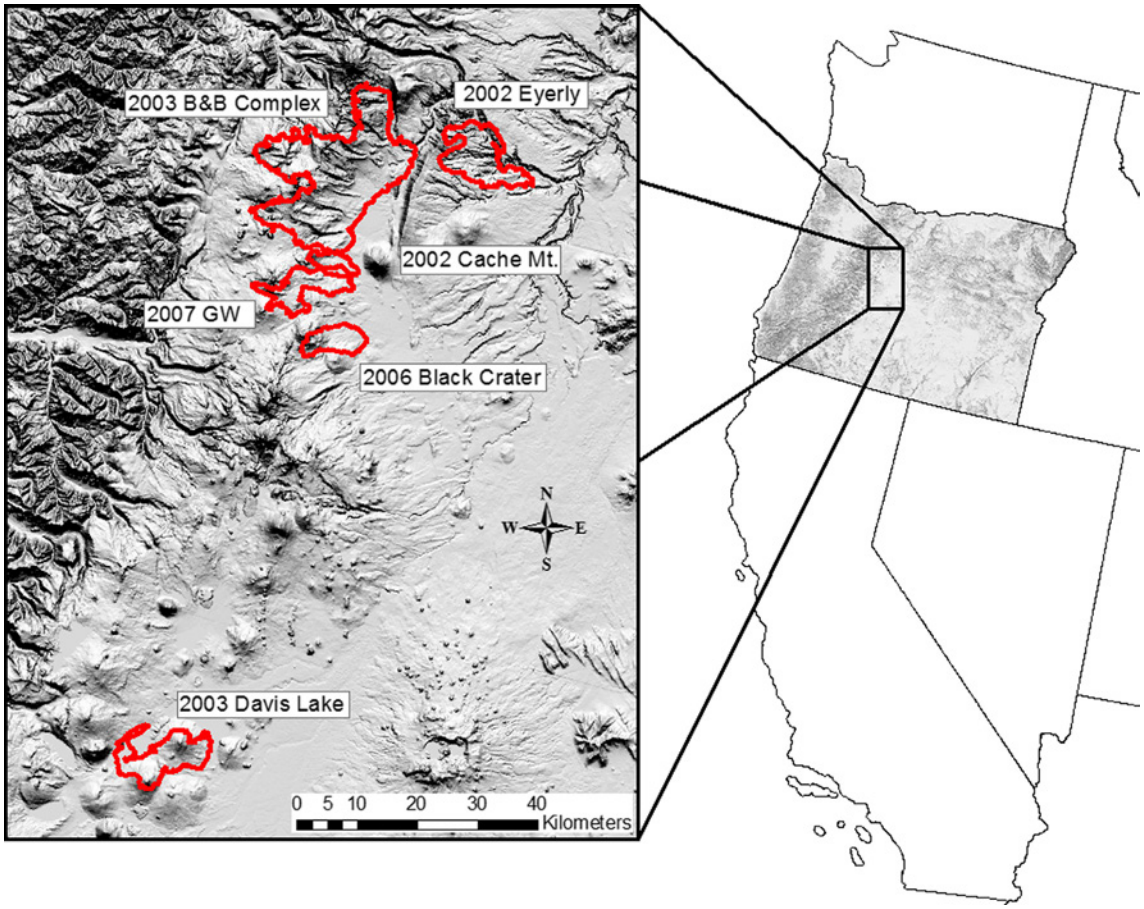

Fig. 2. A map depicting the location of the six fires used in our analysis that burned primarily in ponderosa pine and dry mixed conifer forests in Oregon's eastern Cascade Mountains.

Table 1
Characteristics of six fires used in this study.

			Proportion of area by severity class		
Fire	Year	Size (ha)	Low	Moderate	High
Eyerly	2002	8987	0.31	0.30	0.39
Cache Mt.	2002	1586	0.47	0.42	0.11
Davis Lake	2003	8352	0.16	0.18	0.65
B&B Complex	2003	36,832	0.34	0.25	0.41
Black Crater	2006	3825	0.24	0.52	0.24
GW	2007	2874	0.36	0.34	0.30

annualized Landsat TM time-series maps from 1984 to 2010 at 30 m resolution. For this analysis imputation was based on Euclidian distance in multivariate space derived from Canonical Correspondence Analysis (CCA) (after Ter Braak, 1986), a direct ordination technique. GNN data has been applied to broad-scale vegetation mapping across a wide range of forest ecosystems for multiple objectives (e.g. Ohmann et al., 2012, Davis et al., 2015, Reilly et al., 2018). Complete details on the GNN mapping method are available in Ohmann et al. (2012).

2.3. Fire severity and mortality models

We extracted burn severity maps for the six fires from a mosaicked set of Landsat TM images from 1984 to 2011 processed using the Landtrendr algorithm (Kennedy et al., 2010; Reilly et al., 2017). Landtrendr is a temporal and spatial normalization process using a segmentation algorithm to smooth spectral reflectance of individual pixels through time. This process removes noise associated with variability in atmospheric or phenological conditions common in Landsat scenes with different Julian dates. The normalized image stacks were mosaicked to annual composite normalized burn ratio (NBR) grids and we calculated RdNBR for each year using pre-fire (year −1) and post-fire (year + 1) to ensure Landsat scenes represented an image before and after the fire event.

We developed individual tree mortality models for 21 tree species in response to a fire severity gradient. Our sample included 21,513 trees from 304 plots with pre- and post-fire field observations from the Current Vegetation Survey (CVS) inventory of USDA Forest Service Region 6 (Table 2). The CVS is a systematic regional inventory administered by the USDA Forest Service in Oregon and Washington with the first measurement from 1992 to 1997 and the second from 1997 to 2007 (Max et al., 1996). Field crews sampled these plots at various times pre- and post-fire, so we only used plots with no evidence of a disturbance (except the fire of interest) after the initial plot measurement based on field notes and visual inspection of spectral trajectories from the LandTrendr algorithm described above. We attributed plots, and therefore trees, with a fire severity class based on RdNBR and published fire severity thresholds where < 25%, 25–75%, > 75% basal area mortality were delineated by the RdNBR thresholds where low = < 235, moderate = 235–649, and high = ≥649 severity (Reilly et al., 2017).

2.3.1. Probability of mortality

We estimated the probability of mortality of individual trees using a generalized linear mixed model with a binomial distribution and logit link function. Plot was included as a random effect to account for positive correlations in residuals resulting from spatial autocorrelation of

Table 2
Summary statistics of tree-level data used to quantify probability of mortality for individual species based on diameter at breast height (DBH), fire severity as captured by the relative differenced Normalized Burn Ratio (RdNBR), and number of years after the fire (Years Post-fire) when post-fire plot sampling occurred.

Species	Common name	N	DBH (cm)			RdNBR			Sample time-since-fire
			Mean (SD)	Median	Range	Mean (SD)	Median	Range	Range
Abies amabilis	silver fir	165	26.7 (16.3)	24.6	7.6–82.8	1041.6 (171.6)	1048.3	194.5–1255.7	1–4
Abies concolor	white fir	1022	28.9 (18.4)	25.1	7.6–140.0	573.5 (338.7)	455.5	−11.4 to 1238.2	0–8
Abies grandis	grand fir	1037	27.7 (21.1)	18.5	7.6–111.3	670.3 (397.3)	730.9	−30.7 to 1256.6	0–11
Abies lasiocarpa	subalpine fir	1157	21.8 (13.5)	16.8	7.6–84.6	924.1 (320.8)	1079.0	−7.9 to 1393.9	0–11
Arbutus menziesii	Pacific madrone	565	24.3 (11.6)	22.1	7.6–64.5	462.4 (331.4)	298.0	37.5–1207.6	0–5
Calocedrus decurrens	Incense cedar	336	29.7 (26.6)	18.7	7.6–182.9	614.7 (241.9)	636.4	60.8–1207.6	0–9
Chrysolepis chrysophylla	Giant chinkapin	356	20.9 (13.9)	16.1	7.6–80.0	496.4 (368.8)	488.0	37.5–1207.6	1–5
Chamaecyparis lawsoniana	Port-Orford cedar	113	38.3 (29.0)	33.3	7.6–128.3	679.2 (300.5)	829.6	60.6–969.5	1–3
Larix occidentalis	western larch	229	38.0 (18.7)	37.1	7.6–104.7	516.5 (447.6)	379.4	−52.0 to 1256.6	0–11
Lithocarpus densiflorus	tanoak	2145	19.7 (12.2)	15.5	7.6–113.3	436.3 (369.7)	296.1	37.0–1170.2	0–4
Pinus contorta	lodgepole pine	2501	16.6 (8.6)	14.2	7.6–77.5	654.9 (474.0)	528.6	−52.0 to 1393.9	0–11
Picea engelmannii	Engelmann spruce	1110	33.3 (21.6)	33.4	7.6–126.2	871.2 (361.2)	951.8	−52.0 to 1393.9	0–11
Pinus albicaulis	whitebark pine	233	25.5 (13.1)	22.1	7.9–81.8	702.0 (391.0)	730.3	−7.9 to 1213.4	1–6
Pinus attenuata	knobcone pine	248	19.7 (9.9)	16.1	7.6–50.0	797.9 (294.8)	956.7	42.0–1021.1	1–4
Pinus lambertiana	sugar pine	302	61.0 (44.8)	49.5	7.6–176.3	643.2 (383.4)	648.3	−11.4 to 1207.6	1–9
Pinus monticola	western white pine	461	23.0 (14.0)	18.0	7.6–79.2	752.5 (214.9)	829.6	3.2–1238.2	1–11
Pinus ponderosa	Ponderosa pine	2451	34.5 (24.0)	30.5	7.6–142.5	437.3 (342.2)	395.0	−52.0 to 1238.2	0–13
Pseudotsuga menziesii	Douglas-fir	5668	43.0 (30.5)	37.8	7.6–202.9	500.3 (357.3)	417.8	−52.0 to 1393.9	0–11
Quercus chrysolepis	canyon live oak	851	17.6 (11.1)	13.5	7.6–64.0	507.9 (371.9)	432.7	37.0–1170.2	1–4
Thuja plicata	western redcedar	99	35.1 (20.2)	37.1	7.9–91.4	378.8 (359.1)	219.7	3.2–1135.7	1–5
Tsuga heterophylla	western hemlock	464	29.3 (18.4)	26.0	7.6–110.2	624.1 (383.7)	526.3	3.2–1135.7	1–8

individual trees within plots. We analyzed each species independently and included diameter at breast height (DBH), severity class, and the number of years between the fire and post-fire sample year as fixed-effects. We also tested 2-way interactions among these variables. We report all 21 species we had enough data for even if they were not present in our study area. We conducted these analyses using the lme4 package in R v 3.1.1 (Bates et al., 2015, R Development Core Team, 2014).

2.4. Temporal snag dynamics

We use an existing database of post-fire snags from a 24-year chronosequence and the NecroDynamics model to capture snag fall and fragmentation (Dunn and Bailey, 2015). However, we updated the model by substituting continuous DBH data for DBH classes (Dunn and Bailey, 2012). We estimated the probability of snag fall and snag fragmentation from 6055 and 4458 individual sample records, respectively. We used a generalized linear mixed model with characteristics identical to those described in our mortality model. Although analyzed on continuous data, we present results for three different snag sizes to simplify our presentation of results regarding the effects of DBH and time on snag dynamics.

We used our updated statistical estimates and the NecroDynamics model to quantify changes in snag conditions across a 50-year modeling horizon. We only had estimates of snag dynamics for ponderosa pine, Douglas-fir, grand/white fir, and lodgepole pine so we coerced all other species into one of these four species based on similarities in physical characteristics and wood density. We modeled all true firs, *Calocedrus decurrens* (incense-cedar), *Thuja plicata* (western redcedar) and *Larix occidentalis* (western larch) using grand/white fir estimates, hardwoods, *Pinus albicaulis (whitebark pine)* and *Tsuga mertensiana* (mountain hemlock) with lodgepole pine estimates, and *Pinus monticola* (western white pine) using ponderosa pine estimates. We assume snag dynamics were consistent across post-fire topographic conditions, and use the same fall and fragmentation rates for all severity conditions because estimates are not available for lower fire severity classes. We also assume the trends developed from the 24-year chronosequence are relevant to 50 years since we currently lack estimates extending that far into the future.

2.5. Snag hazard

We were interested in developing a hazard rating system to simplify pixel-level conditions across the post-fire landscapes. To date, no quantitative measure of snag hazard exists so field personnel evaluate hazardous trees during fire management operations. Therefore, we develop our methodology from the authors firefighting experience, consultation with current responders, and field plots of current forest conditions. We focus on snags ≥ 20 cm DBH and derive our hazard rating from snag height (potential reach) and density because these variables directly influence the probability of a snag striking a fire responder. We estimated pre-fire median snag density and height from all 2411 different plots, weighted by their abundance across all six landscapes, as the typical operating environment that sets the threshold of acceptable risk by fire responders. We used medians instead of means as our measure of central tendency to reduce the influence of plots from the 2003 B&B Complex and 2007 GW fires impacted by western spruce budworm (*Choristoneura occidentalis* Freeman) where tree mortality may have resulted in snag densities exceeding the typical operating environment. Pre-fire median snag density was 30 snags ha^{-1} and median height was 13.9 m for snags > 20 cm DBH. We expanded the hazard-rating matrix from these estimates and categorized pixel-level snag conditions into one of four hazard categories with a nomenclature following the Department of Homeland Security rating system (Fig. 3).

We attributed our spatial and temporal datasets with the hazard rating and report summary statistics by fire severity class and incident. We created post-fire snag lists by applying our mortality model to pre-fire tree lists, imputed using the GNN method, at each pixel within the burned landscape. Each tree within the pre-fire tree list was subject to mortality based on the pixels RdNBR value and individual tree attributes as per our mortality model. This creates post-fire snag lists for each pixel across the landscape that change with time based on our snag dynamics results. Then we attributed each pixel, for each year of analysis, with the appropriate snag hazard rating based on their snag density and height. We extracted snag density, median snag height and the hazard rating from each pixel across the six-burned landscapes by severity class, for each year of modeling, to quantify temporal variation in snag hazard associated with fire severity. We then quantified the median snag density and median snag height, as well as the first and third quartiles, and the proportion of pixels in each of the four hazard

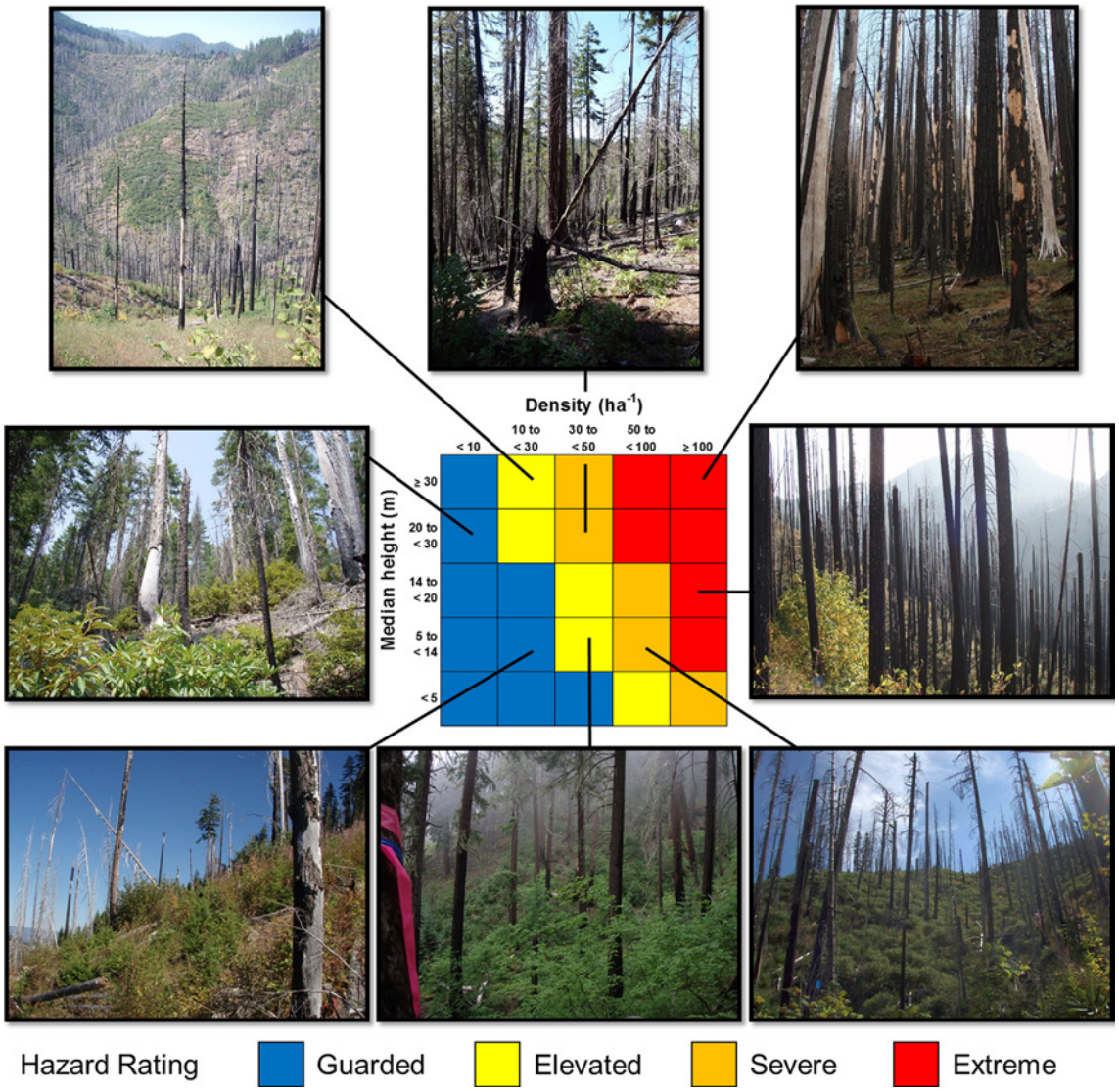

Fig. 3. The snag hazard-rating matrix based on median snag height and snag density. The median snag density across the six fires used in our analysis was 30 snags ha^{-1}, with a median height of 13.9 m. We built the rating system from those values, assuming they represent acceptable conditions in fire management.

ratings for the entire dataset. Then we calculated proportion in each severity class by fire incident to evaluate differences at the fire scale. We also quantified absolute maximum patch size for severe and extreme conditions combined, as well as the proportion of total burned area consisting of these two most severe hazard classes. We did this on an annual basis across the 50-year modeling horizon for each incident using ClassStats function in the SDMTools package in R (VanDerWal et al., 2014). We combined these hazard ratings because they both represent enough risk to fire responders that they warrant alternative engagement strategies or tactics.

3. Results

3.1. Probability of mortality

We were able to create statistical models estimating the probability of mortality for 21 species of conifer and hardwoods trees found in the Pacific Northwest. Table 3 contains the statistical models and significance of covariates for each species. We also include three figures as online supplemental material depicting the response of fire-tolerant, fire-intolerant and hardwood trees by severity class across their observed DBH range. As expected, the probability of mortality increased with increasing fire severity for all species, but the magnitude of difference by fire-severity class and relationships with DBH varied by species.

Our analysis indicates a decreasing probability of mortality with increasing DBH for species commonly considered fire-tolerant, including Douglas-fir, ponderosa pine, western larch, sugar pine and white fir. The only exception was incense-cedar where DBH did not have a statistical correlation with probability of mortality (Table 3). We considered white fir to be fire tolerant because it develops thick bark in this region, especially at larger diameters. Hardwood species had a similar response, but generally exhibited a higher likelihood of mortality than fire-tolerant conifers. An interaction term between DBH and fire severity was statistically significant for Douglas-fir and ponderosa pine, indicating different response slopes. Additionally, we observed a statistically significant relationship with the number of years post-fire when re-measurement occurred, indicating delayed mortality for Douglas-fir, canyon live oak, and tanoak. For modeling purposes, we attribute tree mortality up to 10-years post-fire (or maximum number of years sampled post-fire, whichever is smaller) as fire-related and capture them in our models when quantifying tree mortality across the burned landscapes.

In contrast, the majority of species commonly considered fire-

Table 3
Statistical results (mean and (standard errors)) for probability of mortality by species, diameter at breast height (DBH), fire severity class (low, moderate and high), number of years after the fire (Years Post-fire) when post-fire plot sampling occurred, and interactions among DBH and fire severity.

Species	Common Name	Intercept	DBH (cm)	Moderate-severity	High-severity	Years Post-fire	DBH*Moderate	DBH*High
Abies amabilis	silver fir	0.000 (1.414)		2.197 (1.764)	3.912 (1.530)*			
Abies concolor	white fir	1.259 (0.623)*	−0.039 (0.006)***	1.625 (0.748)*	5.636 (0.999)***			
Abies grandis	grand fir	0.807 (0.464)***	−0.029 (0.005)***	1.450 (0.581)*	5.200 (0.755)*			
Abies lasiocarpa	subalpine fir	0.356 (0.936)		1.972 (1.113)	4.467 (1.087)***			
Arbutus menziesii	Pacific madrone	1.616 (0.690)*	−0.099 (0.015)***	1.056 (0.811)	4.221 (1.026)***			
Calocedrus decurrens	Incense cedar	−1.134 (0.756)		1.867 (0.923)*	4.020 (1.050)***			
Chrysolepis chrysophylla	Giant chinkapin	1.372 (0.604)*	−0.104 (0.020)***	2.735 (0.854)**	6.088 (1.395)***			
Chamaecyparis lawsoniana	Port-Orford cedar	1.378 (1.133)	−0.037 (0.011)**		4.180 (1.136)***			
Larix occidentalis	western larch	−0.088 (1.348)	−0.072 (0.021)**	4.025 (1.617)*	8.550 (2.133)***			
Lithocarpus densiflorus	tanoak	−0.378 (0.700)	−0.101 (0.008)***	1.324 (0.607)*	5.825 (0.895)***	0.902 (0.304) **		
Pinus contorta	lodgepole pine	0.869 (0.506)	−0.030 (0.009)***	1.293 (0.614)*	4.624 (0.684)***			
Picea engelmannii	Engelmann spruce	0.277 (1.361)		2.230 (1.680)	5.950 (1.721)***			
Pinus albicaulis	whitebark pine	−3.466 (1.102)***		3.800 (1.052)***	6.306 (1.079)***			
Pinus attenuata	knobcone pine							
Pinus lambertiana	sugar pine	0.559 (0.722)	−0.022 (0.006)***	0.532 (0.831)	4.203 (0.967)***			
Pinus monticola	western white pine	−0.510 (1.053)		1.090 (1.500)	4.780 (1.252)***			
Pinus ponderosa	ponderosa pine	−1.588 (0.380)***	−0.014 (0.005)**	2.967 (0.512)***	7.144 (0.755)***		−0.017 (0.007)*	−0.030 (0.009)**
Pseudotsuga menziesii	Douglas-fir	−0.788 (0.369)*	−0.037 (0.004)***	0.818 (0.405)*	4.363 (0.464)***	0.256 (0.071)***	0.013 (0.005)**	0.014 (0.005)**
Quercus chrysolepis	canyon live oak	−0.854 (0.837)	−0.091 (0.015)***	1.446 (0.633)*	5.495 (0.931)***	0.627 (0.310)*		
Thuja plicata	western redcedar	−1.966 (0.585)***		0.817 (1.159)	1.328 (0.662)*	0.619 (0.171)***		
Tsuga heterophylla	western hemlock	0.878 (0.783)	−0.027 (0.011)*	2.872 (1.171)*	4.631 (1.307)***			
Tsuga spp.	hemlock	0.564 (0.798)	−0.027 (0.011)*	3.774 (1.221)**	5.662 (1.124)***			

Note: P-values for categorical variables represent statistical comparisons to low-severity fire.
Note: Estimates are means and standard errors in parentheses.
* p-value ≤ 0.05.
** p-value ≤ 0.01.
*** p-value ≤ 0.001.

Table 4
Statistical results for snag fall and fragmentation rates as a function of time-since-fire, species (reference group is grand fir, PICO = lodgepole pine, PIPO = ponderosa pine, PSME = Douglas-fir), and diameter at breast height (DBH).

Snag fall rates				
Fixed effects:	Estimate	Std. Error	z-value	Pr(> |z|)
Intercept	−2.975	0.239	−12.448	< 0.001
Time-since-fire (yrs)	0.355	0.027	13.366	< 0.001
PICO	0.137	0.615	0.223	0.824
PIPO	1.660	0.286	5.798	< 0.001
PSME	0.480	0.325	1.474	0.141
DBH (cm)	−0.057	0.004	−14.278	< 0.001
Time*PICO	0.129	0.096	1.352	0.176
Time*PIPO	−0.088	0.030	−2.936	0.003
Time*PSME	−0.131	0.045	−2.881	0.004
AIC	BIC	logLik	deviance	df.resid
5090.3	5157.4	−2535.1	5070.3	6045
Random effects:	# of obs: 6055		# of groups: 30	
	Groups:		Variance	Std.Dev.
	plots	Intercept	0.453	0.673
Snag fragmentation rates				
Fixed effects:	Estimate	Std. Error	z-value	Pr(> |z|)
Intercept	−5.520	0.369	−14.945	< 0.001
Time-since-fire (yrs)	0.225	0.038	5.899	< 0.001
PICO	1.394	0.794	1.756	0.079
PIPO	3.604	0.314	11.478	< 0.001
PSME	0.814	0.270	3.020	0.003
DBH (cm)	0.085	0.006	14.847	< 0.001
DBH*PICO	−0.105	0.052	−2.031	0.042
DBH*PIPO	−0.095	0.008	−12.513	< 0.001
DBH*PSME	−0.048	0.008	−5.722	< 0.001
AIC	BIC	logLik	deviance	df.resid
2162.8	2226.8	−1071.4	2142.8	4448
Random effects:	# of obs: 4458		# of groups: 30	
	Groups	Name	Variance	Std.Dev.
	plots	Intercept	1.207	1.099

intolerant did not exhibit statistically significant correlation with DBH, suggesting they do not develop increased fire tolerance with increasing size (Table 3). The exceptions were grand fir, lodgepole pine and western hemlock. Unexpectedly, grand fir estimates were nearly equivalent to white fir, a species commonly thought to be more fire-tolerant, which may be a function of hybridization in our study area. These fire-intolerant species exhibit higher likelihood of mortality in all severity classes, with zero or few individuals surviving high-severity fire. In many cases, the differences between fire severity classes were low as indicated by overlapping error bars (see online supplemental material). Only western redcedar had a statistically significant relationship with the number of years post-fire when re-measurement occurred, suggesting they too exhibit measureable delayed mortality that is accounted for in our modeling as described previously.

3.2. Temporal snag dynamics

The cumulative probability of snag fall increased with the number of years-since-fire, and varied by species and DBH (Table 4). Larger snags were more likely to remain standing than smaller snags across all species, with Douglas-fir having the lowest probability of falling (Fig. 4). The interaction term between species and years-since-fire was statistically significant as the slopes of the trend lines varied. Half-life estimates (i.e. year when 50% of the snag population has fallen) provide a metric for comparing fall rates across populations of interest and among studies. Half-lives for small ponderosa pine snags (20 cm DBH) were 9–10 years, medium snags (40 cm DBH) were 13–14 years, and large snags (80 cm DBH) were 22–23 years. Half-lives for small lodgepole pine snags were 8–9 years and 10–11 years for small and medium snags, respectively. We did not encounter large lodgepole pine snags in our sample. Half-lives for small grand/white fir snags were 11–12 years, medium snags were 14–15 years, and large snags were 21–22 years. Lastly, half-lives for small Douglas-fir snags were 16–17 years, medium snags were 21–22 years, and large snags were 31–32 years. Table 4 provides coefficients for the significant predictor variables and random error terms for estimating the cumulative probability of fallen snags on the logit scale. The plot random error term was statistically significant, indicating additional environmental effects influence snag fall at that scale (e.g. wind events).

The cumulative probability of snag fragmentation increased with time-since-fire, but varied by species and DBH. We also observed an interaction between DBH and species (Table 4). In general, the relationship with DBH and time was opposite that for fall rates as larger snags were more likely to fragment. However, we observed little variation by diameter for lodgepole and ponderosa pine. Ponderosa pine generally had the highest fragmentation rates with exception of the large grand/white fir that also fragmented rapidly (Fig. 4). The majority of smaller DBH snags fell before fragmenting. Table 4 provides coefficients for the significant predictor variables and random error terms for estimating the cumulative probability of snags with broken tops on the logit scale. We estimated changes in snag height over time from the same data and included in the NecroDynamics model. We encourage those interested in more details regarding snag dynamics to review Dunn and Bailey (2012, 2015).

3.3. Snag hazard

We observed a positive relationship between fire severity and median snag density and height as more and larger trees were killed (Fig. 5). Median snag density (1st and 3rd quartile) was 38 (14, 90), 127 (69, 215) and 241 (153, 383) snags ha^{-1} immediately following low, moderate and high-severity fire, respectively. Median snag height was 16.1 (12.8, 19.8), 17.4 (14.1, 20.4), and 18.6 (16.0, 21.3) immediately following low, moderate and high-severity fire, respectively. These snag conditions resulted in an increasing proportion of higher hazard ratings as fire severity increased. For low-severity fire areas, 29%, 18%, 14% and 39% had a hazard rating of extreme, severe, elevated and guarded, respectively. Following moderate-severity fire, 66%, 17%, 6% and 10% had a hazard rating of extreme, severe, elevated and guarded, respectively. After high-severity fire, 86%, 5%, 3% and 6% had a hazard rating of extreme, severe, elevated and guarded, respectively. As fire severity increased so too did the time that severe and extreme hazard conditions persisted. Low-severity fire areas retained some severe and extreme conditions for up to 20 years, moderate-severity up to 30 years, and high-severity up to 35 years. It is also important to note that the rapid decline in snag abundance began around 10 years post-fire and lasted until 20 to 25 years post-fire depending on fire severity (Fig. 4). This represents the period of highest risk directly attributed to snag fall and fragmentation, exclusive of the effects of burning again which would accelerate fall or fragmentation.

The spatial and temporal variation in snag hazard across fire incidents depends on interactions among fire-severity and pre-fire stand structure (Fig. 6). Fires with the largest area and longest duration with a severe or extreme hazard rating were the 2003 B&B Complex and 2003 Davis Lake fires that also had the highest proportion of high-severity fire (Table 1). In contrast, the 2002 Eyerly fire also burned with a high-proportion of high-severity relative to the other fires in our sample, but much of the landscape was non-forested. We included pre-fire estimates of hazard ratings as well, recognizing that fire is not the only disturbances affecting these forests. The effects of western spruce budworms within the 2003 B&B Complex and 2007 GW fires prior to burning are evident in the western portion of their burned area. We include maps of the 2003 B&B Complex to demonstrate temporal and spatial change across a burned landscape (Fig. 7). The relationship between fire severity and snag hazard becomes evident later in the time-series. We include additional annual time-series maps of snag

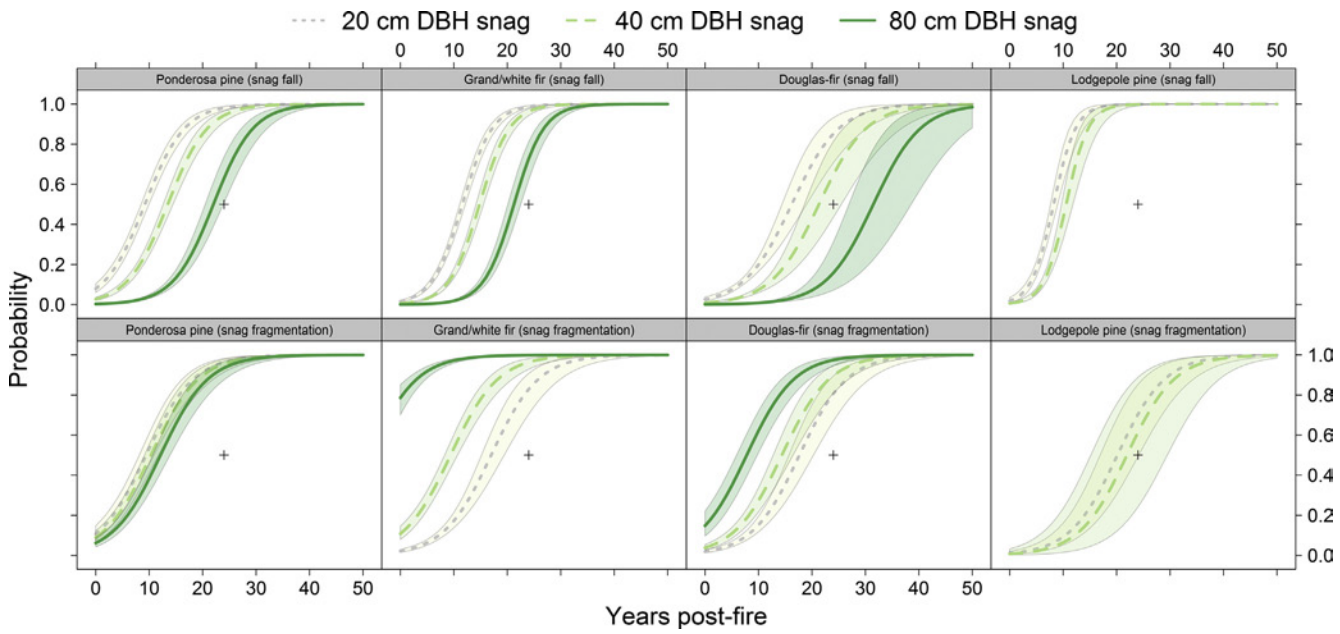

Fig. 4. Probability of snag fall and fragmentation by species for three different DBH snags (20 cm, 40 cm, and 80 cm DBH). Higher slopes represent an increase in risk of injury or death from snag fall or fragmentation. The plus sign was placed at a 0.5 probability and 24 years post-fire for reference. 24 years was the oldest sample year in this chronosequence, although we project to 50 years.

hazard for multiple fires as online supplemental material.

The characteristics of each incident influenced the absolute patch size of combined severe and extreme hazard, as well as the proportion of burned area covered by that patch. Fire size had the greatest relationship to absolute patch size (Fig. 8), amounting to 24,807 ha immediately following the 2003 B&B Complex fire. The B&B Complex's maximum patch size was 3.75 times that of the second ranked 2003 Davis Lake fire in our sample (B&B Complex was 4.41 times the total extent of the Davis Lake fire). However, fire size was not the only important factor as fire severity, pre-fire forest structure and composition played an important role, particularly concerning temporal trends. For example, the 2003 Davis Lake fire had the highest proportion (0.65) of high-severity fire among all fires investigated. Davis Lakes' high-severity areas primarily formed as a single contiguous patch that directly translated into the highest single patch of severe or extreme snag hazard (79.1% of the burned area). A review of the pre-fire forest structure and composition showed that much of the Davis Lake high-severity patch burned through old-growth stands with large trees. These snags stand longer (Fig. 4), and combined with the large contiguous patch of high-severity fire, resulted in the Davis Lake fire's maximum patch size being the most persistent and eventually largest over time (Fig. 8). In contrast, the 2002 Eyerly fire contained significant area of non-forest vegetation, breaking up the patches of severe and extreme snag hazard such that only 24.0% of the burned area was in a single contiguous patch. Immediately following the 2002 Cache Mt. fire with the lowest overall fire severity, only 27.2% of the burned area formed a contiguous patch of severe or extreme snag hazard rating.

4. Discussion

In this study, we demonstrated a methodology for characterizing and mapping snag hazard to fire responders in recently disturbed forests (Fig. 1). We were able to map snag hazard across burned landscapes by integrating pre-fire remote-sensing, field inventories, and imputation based vegetation modeling with empirically derived mortality models. Subsequently, we projected the spatial distribution and magnitude of snag hazards into the future using the recently developed NecroDynamics model (Dunn and Bailey, 2015). This process demonstrates how interdisciplinary collaboration can further our adaptation to future fire and climate change, in part by recognizing the importance of the fire management system in addressing these challenges (Thompson et al., 2015; 2018). Our results offer important insights regarding the consequences of dynamic snag hazard on near and long-term wildfire risk.

Snag hazard increases significantly in post-fire environments and may be creating novel management challenges not encountered over the past 50+ years. Hazardous fuel, stand densities, and susceptibility of trees to death from fire has increased over the past 100+ years as the consequences of past forest and fire management policies and practices interact with warmer, drier conditions that promote more extreme fire behavior in denser forest environments (Naficy et al., 2010; Stephens et al., 2014; Jolly et al., 2015). Fire severity is higher than observed historically in many forest types, resulting in more and larger diameter snags than encountered when Euro-American colonization altered disturbance regimes with an aggressive fire suppression paradigm (Johnston et al., 2018.) (Fig. 5). High snag densities and larger snags with a greater fall-reach, wider crowns, and greater mass increase responder exposure to this hazard. Larger snags also persist longer on the landscape (Fig. 4), increasing the probability that another ignition will occur within a severe or extreme snag hazard area. Furthermore, the onset of large or mega-fires in recent decades increases the overall extent of burned landscapes (Stephens et al., 2014), including the absolute patch-size of high-severity fire (Reilly et al., 2017; Stevens et al., 2017). Given the relationship between fire size, patch-size, fire severity and snag hazard (Figs. 5 and 8), we are likely to continue to observe an increase in responder exposure to snag hazard into the future. Insect outbreaks (e.g., bark beetles), drought, and other non-fire mortality factors compound these conditions across many forest types (Meddens et al., 2012; McDowell et al., 2015).

Snags directly affect safe and effective wildfire response during all stages of incident management. First responders may not be able to engage directly with an ignition because of snags, especially when they are on fire. Burning increases the likelihood that all or a portion of a snag will fall, reducing opportunities to extinguish the fire immediately. Fire responders may have to wait until the burning snag falls before constructing a containment line around it. Accessing the point of ignition may require travel through hazardous areas (Fig. 8), further exposing responders to injury or death. Therefore, pursuing alternative

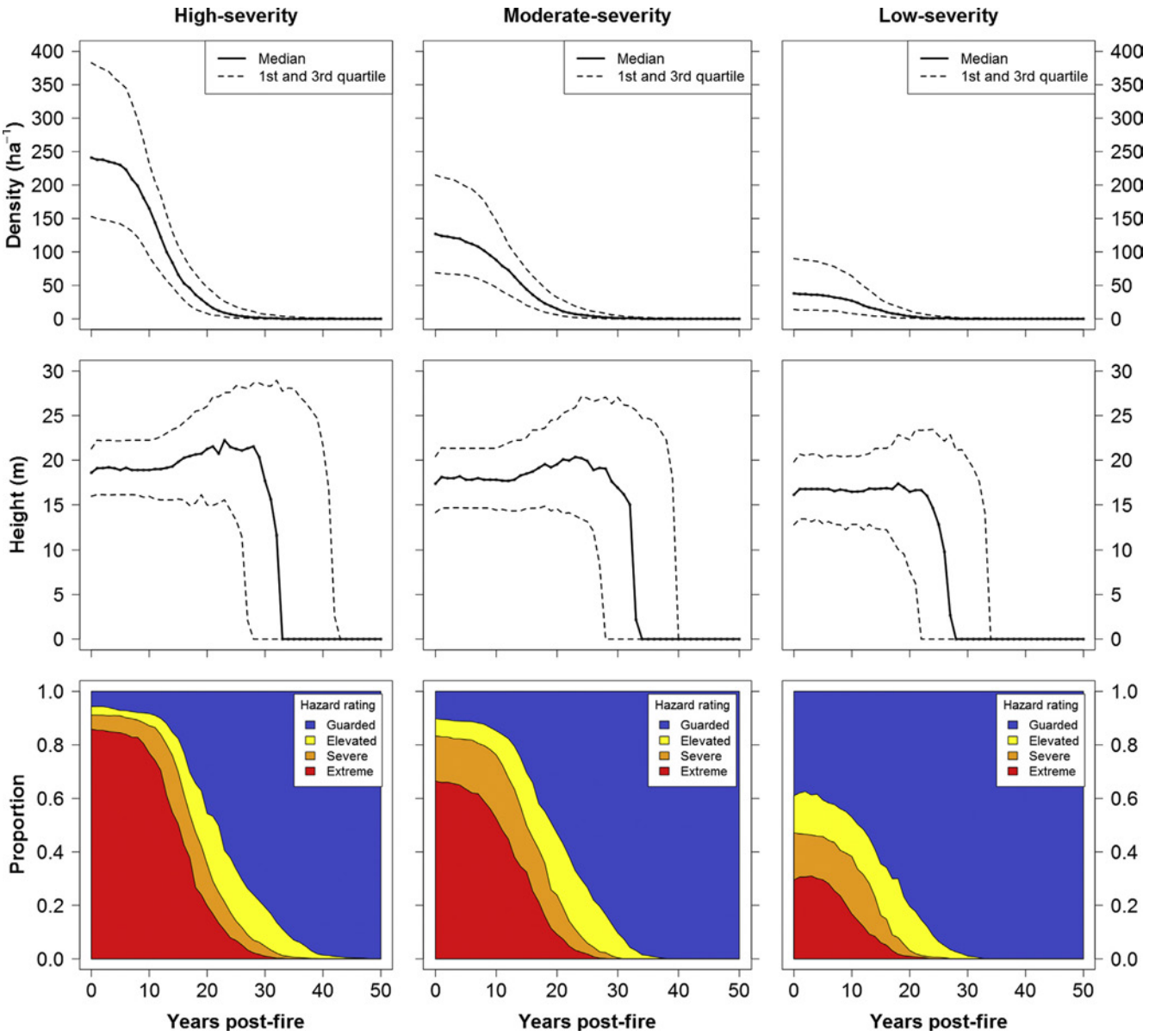

Fig. 5. Summary of snag characteristics and hazard by severity class. We present median snag density and height, and first and third quartiles for variability, because of the skewed distribution of these data sets.

response tactics may be necessary and snag hazard maps could help facilitate more rapid risk-informed decisions.

Hazardous snag conditions also affect large fire response strategies and tactics. Desired control lines may fall within a previously burned area with a severe or extreme snag hazard rating. Pursuing a strategy that uses this control line would require extensive hazard mitigation that consumes time and resources while increasing responder exposure. These conditions may also compromise escape routes and safety zones, and increase responder exposure during mop-up since fire weakens snags. In fact, responders often spend extensive time mopping up a fire as much as 90 m inside a control line, where snags > 150 m inside the control line are a threat. Mapping snag hazard, and overlaying it with potential control locations (O'Connor et al., 2017) could help fire managers make risk-informed strategic response decisions that balance responder exposure with likelihood of containment success.

Opportunities to mitigate snag hazard during an incident may be limited across much of the landscape because of an abundance of snags and their felling complexity. Felling snags is more complex than live trees because of uncertainty in holding wood strength, the distribution of weight throughout the snag, and the potential for tops to break during cutting. Exposing responders to this hazard elevates risk of injury or death, leaving avoidance as the less risky mitigation strategy. This could amount to avoiding large portions of a landscape (Fig. 7), particularly after 10 years when reburn becomes more likely and snag fall rates increase (Collins et al., 2009; Parks et al., 2015). In fact, our estimates suggest > 20,000 ha, or 60% of the burned landscape in our largest sampled fire at 10 years post-fire, may have conditions where exposure outweighs the benefits of engagement (Fig. 8). Mapping snag hazard as we have done here improves situational awareness for both decision makers and fire responders during strategic response development and the ensuing tactical response.

4.1. Long-term wildfire risk management

Risk management and risk sharing provide important foundational principles and practices for long-term wildfire risk reduction (Dunn et al., 2017a). Risk management (RM) is a set of coordinated processes and activities that identify, assess, monitor, prioritize, and control risks

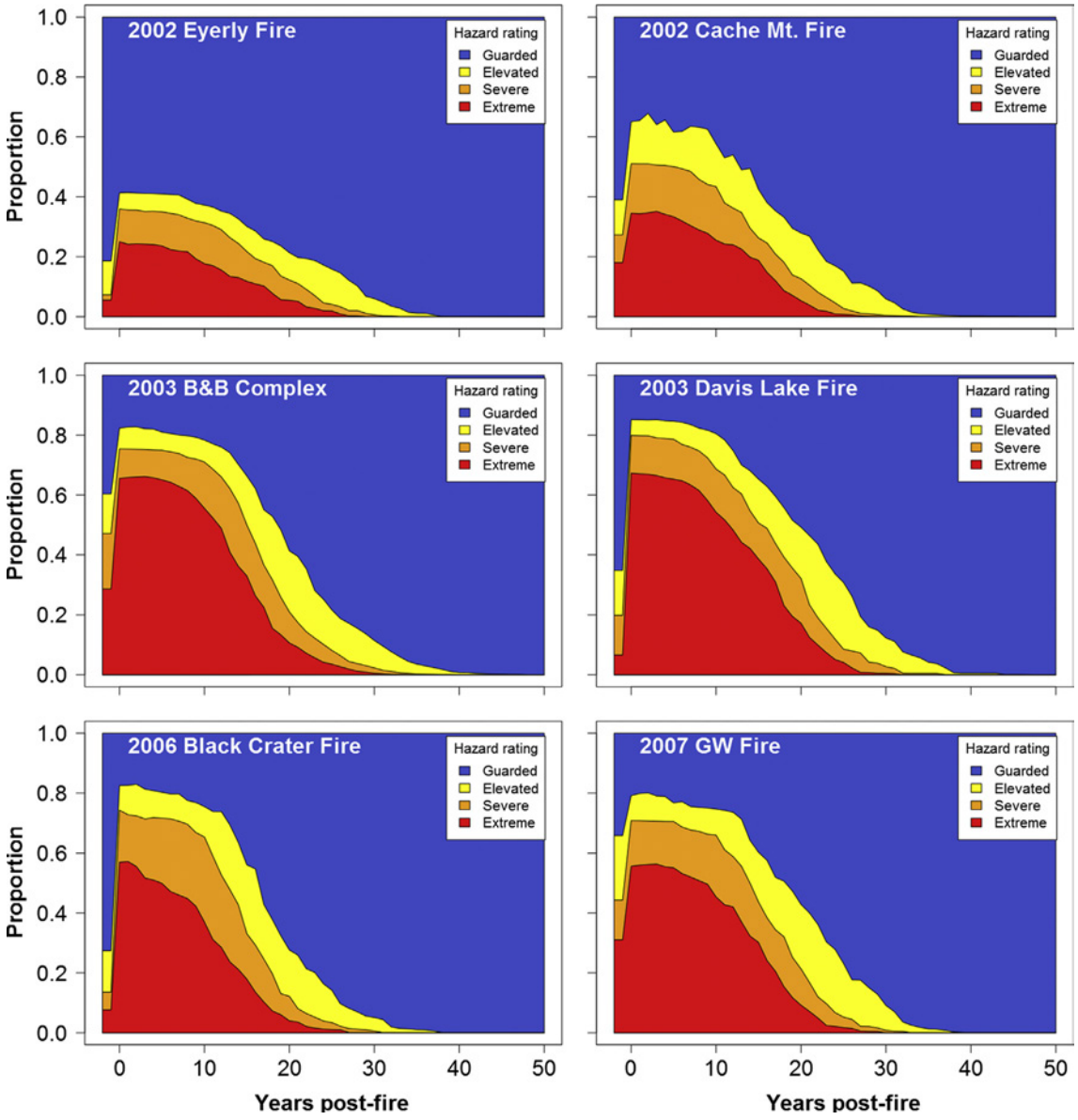

Fig. 6. Temporal trends in snag hazard for six fires represented as the proportion of landscapes in each of the hazard rating classes.

that an organization does or will face. RM considers high-impact to mundane decisions, and spans organizational to individual actions before, during, and after these decisions. RM also involves assessment and planning well in advance of decisions and shares risk management responsibility throughout the organizational structure (Thompson et al., 2016a, 2016b). Implementing such comprehensive wildfire risk management would align land management objectives and actions such that they support wildfire response (Dunn et al., 2017b). This is particularly important since managing the existing wildfire threat and implementing viable mitigation options relies heavily on the fire management system and its ability to overcome the wildfire paradox (Thompson et al., 2015). The wildfire paradox suggests positive feedbacks from negative consequences of wildfires reinforce aggressive suppression, despite this strategy contributing to and perpetuating the existing problem. Until now, the real or perceived negative consequences from wildfires on ecosystem resilience (Stevens-Rumann et al., 2018) and social resources and assets (Charnley et al., 2017) were considered the drivers of the wildfire paradox (Calkin et al., 2015). We have demonstrated that responder exposure to snag hazard may further entrench the wildfire paradox as fire managers consider the negative consequences of large fires on future responder risk, especially in the absence of other remediation. As fires accumulate across landscapes fire responders may be forced to overcome the paradox as recently burned landscapes ignite again and snag hazard leads to a less aggressive initial response to minimize risk, unless political pressure leads to increasingly risky behavior (Canton-Thompson et al., 2008). Fortunately, there are options for proactive management actions with direct and measureable benefits achieved as risk management aligns across land and fire management agencies and activities.

Land managers historically addressed hazardous snags in post-fire environments via extensive salvage logging. However, economic, ecological, logistical and administrative constraints limit the spatial extent and locations available for active management (North et al., 2015). From an enterprise risk management perspective, salvage logging also transfers risk from fire responders to timber harvesters, a more hazardous trade (Center for Disease Control and Prevention, 2018), and is a reactive action addressing symptoms rather than root causes. An alternative is targeted treatments along potential control locations (O'Connor et al 2017), which could break up the severe or extreme snag hazard landscape (Fig. 8), supporting safe and effective response by

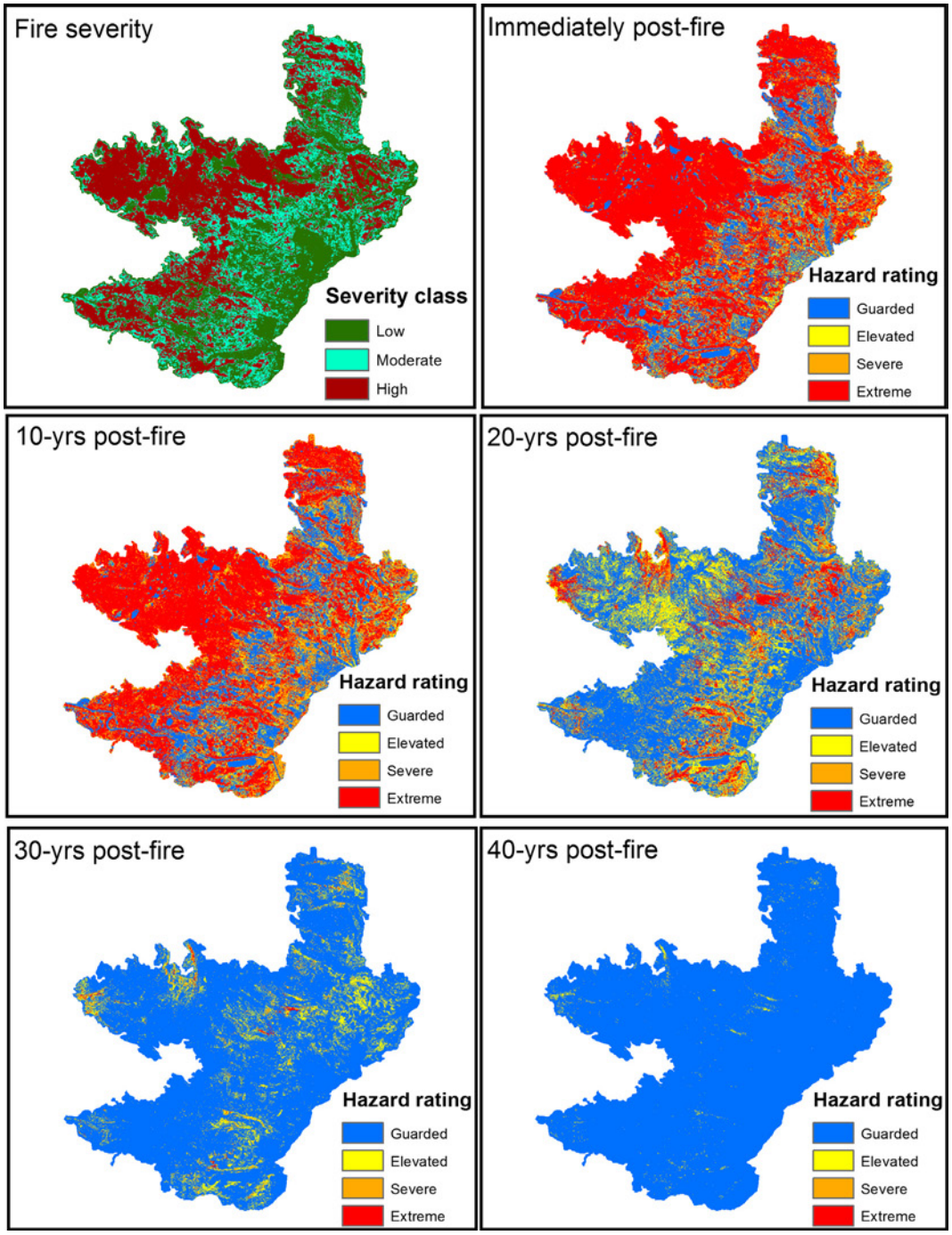

Fig. 7. Spatial and temporal change in snag hazard for the 2003 B&B Complex. The first panel depicts fire severity while the remaining depict snag hazard at increasing time since fire. The decadal period of highest hazard was between 10 and 20- years, although significant hazard persists through 30 years following high-severity fire.

minimizing exposure while reinforcing the most likely large fire containment lines.

Proactive management actions can address the root causes of increased snag hazard in post-fire environments. Forest restoration or hazardous fuels reduction reduces tree density and decreases tree mortality by increasing the fire tolerance of residual trees while reducing fire intensity (Agee and Skinner, 2005). These treatments are limited by the same constraints noted previously, so prescribed fire or managing wildfires for resource objectives may be the most effective strategy for achieving these fuels reduction benefits. Wildfires burning during low and moderate fire weather conditions would promote lower severity fire, reducing the abundance and patch-size of severe and extreme snag hazard (Figs. 5 and 8). Prescribed fire and managing wildfires for resource objectives could be extended to the post-fire environment with a burn-the-burn strategy, especially in low- and moderate-severity areas. Doing so could minimize the probability of fire occurrence in high-severity fire areas by inhibiting fires spread into them, while also helping to contain a fire ignited within. Reburning landscapes also reduces snag hazard in the short and long-term by increasing fall rates of existing snags, and preventing the development of forest conditions that exacerbate snag hazard in post-fire environments. Ultimately, aligning land management decisions with more of the "right" kind of fire in the "right" places at the "right" time with the goal of reducing risk to ecosystems and their services, social assets and

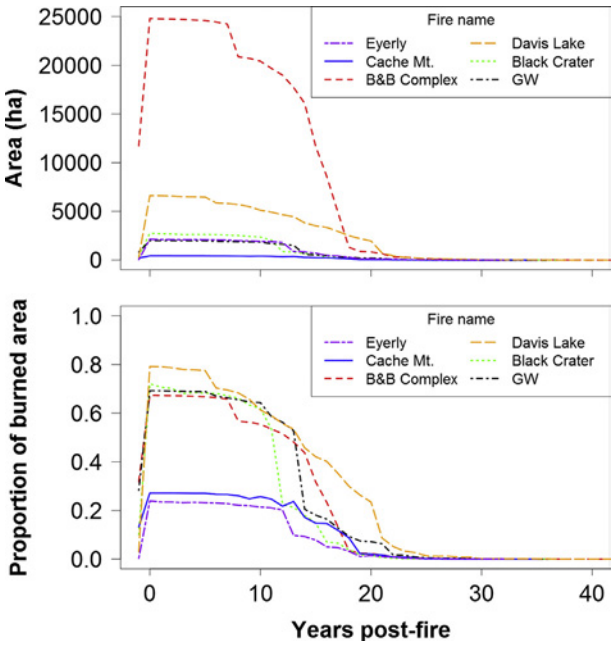

Fig. 8. Maximum patch size of combined severe and extreme snag hazard for each fire modeled across a 50-year modeling horizon, depicted as absolute size and proportion of the landscape.

property, and fire responders will help transition to a new fire management paradigm that produces desirable long-term outcomes in fire-prone landscapes.

4.2. Future needs

In this manuscript, we described a methodology for assessing and mapping snag hazards in post-fire environments, and in so doing, discovered new perspectives on the implications of contemporary wildfire effects. However, our research goals are to provide decision support tools that improve the safety and effectiveness of wildfire management. Doing so requires additional research investment and expansion of our methodologies across a broader geographic scale. First, we need to expand our mortality model to include additional species across a variety of ecoregions. The Forest Inventory and Analysis (FIA) program's field plots likely meets this need. Second, we need to add to the growing body of literature on post-fire snag dynamics (Grayson et al., 2019) to stratify across additional tree species, topographic positions, and post-fire stand characteristics. These factors contribute to highly variable snag dynamics not well documented (Dunn and Bailey, 2016), and are particularly important for aligning post-fire land management decisions with fire response in the future. Third, our model requires pre-fire tree lists that include species, DBH and height. Riley et al. (2016) have imputed tree lists from FIA field plots across the western U.S., although they used a different methodology than GNN. Lastly, we need to ensure that our hazard rating system is both quantitatively accurate and representative of how snag hazards influence strategic and tactical decisions. We are currently in the process of surveying fire responders across a broad gradient of incident qualifications to refine our hazard rating system.

We also recognize the need to integrate additional hazards into a single responder exposure index that is actionable for fire responders and informative for land management decisions. Extending our methodology to other forest disturbances (e.g., drought and insects) would contribute to a more comprehensive assessment of responder exposure to snag hazard (Meddens et al., 2012; McDowell et al., 2015). In addition, snags become logs and heavy accumulation of coarse wood elevates resistance to control by impeding travel, reducing line construction rates, and increasing the difficulty of extinguishing a fire (Page et al., 2013). Lastly, obtaining estimates of reburn impacts on snag demographics would help clarify how alternative response strategies mitigate or exacerbate snag hazard in post-fire environments, so that land and fire management decisions most effectively support long-term risk reduction to fire responders. Expanding research to include these factors requires investment, but minimizing risk of injury or death to fire responders is prudent for an organization focused on enterprise risk management, especially as the fire environment becomes increasingly complex.

Conflict of interest

The authors declare no conflicts of interest.

Acknowledgements

Funding for this research came from the Research Joint Venture Agreement No. 15-JV-11221636-059, with the US Forest Service Human Dimensions Program at the Rocky Mountain Research Station.

Appendix A. Supplementary material

Supplementary data to this article can be found online at https://doi.org/10.1016/j.foreco.2019.03.035.

References

Abatzoglou, J.T., Wiliams, A.P., 2016. Impact of anthropogenic climate change on wildfire across western US forests. Proc. Natl. Acad. Sci. 113 (42), 11770–11775.
Agee, J.K., Skinner, C.N., 2005. Basic principles of forest fuel reduction treatments. For. Ecol. Manage. 211, 83–96.
Bates, D., Maechler, M., Bolker, B., Walker, S., 2015. Fitting linear mixed-effects models using lme4. J. Stat. Softw. 67 (1), 1–48. https://doi.org/10.18637/jss.v067.i01.
Bull, E.L., Parks, C.G., Torgersen, T.R., 1997. Trees and Logs Important to Wildlife in the Interior Columbia River Basin. USDA Forest Service General Technical Report PNW-GTR-391. Pacific Northwest Research Station, Portland, OR.
Butler, B.W., 2014. Wildland firefighter safety zones: a review of past science and summary of future needs. Int. J. Wildland Fire 23, 295–308.
Calkin, D.E., Ager, A.A., Gilbertson-Day, J. (Eds.), 2010. Wildfire risk and hazard: procedures for the first approximation. Gen. Tech. Rep. RMRS-GTR-235. Department of Agriculture, Forest Service, Rocky Mountain Research Station, Fort Collins, CO: U.S., pp. 62.
Calkin, D.E., Thompson, M.P., Finney, M.A., 2015. Negative consequences of positive feedbacks in US wildfire management. Forest Ecosystems 2 (1), 1–10.
Campbell, M.J., Dennison, P.E., Butler, B.W., 2017. A LiDAR-based analysis of the effects of slope, vegetation density, and ground surface roughness on travel rates for wildland firefighter escape route mapping. Int. J. Wildland Fire 26 (10), 884–895.
Canton-Thompson, J., Gebert, K.M., Thompson, B., Jones, G., Calkin, D.E., Donovan, G., 2008. External human factors in incident management team decision making and their effect on large fire suppression expenditures. J. Forest. 106 (8), 416–424.
Center for Disease Control and Prevention. 2018. https://www.cdc.gov/niosh/topics/logging/default.html. (access 12-01-18).
Charnley, S., Spies, T.A., Barros, A.M.G., White, E.M., Olsen, K.A., 2017. Diversity in forest management to reduce wildfire losses: implications for resilience. Ecol. Soc. 22 (1), 22.
Collins, B.M., Miller, J.D., Thode, A.E., Kelly, M., van Wagtendonk, J.W., Stephens, S.L., 2009. Interactions among wildland fires in a long-established sierra nevada natural fire area. Ecosystems 12, 114–128.
Davis, R.J., Ohmann, J.L., Kennedy, R.E., Cohen, W.B., Gregory, M.J., Yang, Z., Roberts, H.M., Gray, A.N., Spies, T.A., 2015. Northwest Forest Plan-the First 20 Years (1994–2013): Status and Trends of Late-Successional and Oldgrowth Forests. General Technical Report PNW-GTR-911. USDA Forest Service, Pacific Northwest Research Station, Portland, Oregon, USA.
Dunn, C.J., Bailey, J.D., 2012. Temporal dynamics and decay of coarse wood in early seral habitats of dry-mixed conbifer forests in Oregon's Eastern Cascades. For. Ecol. Manage. 276, 71–81.
Dunn, C.J., Bailey, J.D., 2015. Modeling the direct effects of salvage logging on longterm temporal fuel dynamics in dry-mixed conifer forests. For. Ecol. Manage. 341, 93–109.
Dunn, C.J., Bailey, J.D., 2016. Tree mortality and structural change following mixed-severity fire in Pseudotsuga forests of Oregon's western Cascades, USA. For. Ecol. Manage. 341, 93–109.
Dunn, C.J., Calkin, D.E., Thompson, M.P., 2017a. Towards enhanced risk management: planning, decision making and monitoring of US wildfire response. Int. J. Wildland Fire 26, 551–556.
Dunn, C.J., Thompson, M.P., Calkin, D.E., 2017b. A framework for developing safe and effective large-fire response in a new fire management paradigm. For. Ecol. Manage.

404, 184–196.
Franklin, J.F., Shugart, H.H., Harmon, M.E., 1987. Tree death as an ecological process. Bioscience 37, 550–556.
Grayson, Lindsay M., Cluck, Daniel R., Hood, Sharon M., 2019. Persistence of fire-killed conifer snags in California, USA. Fire Ecol. 15 (1). https://doi.org/10.1186/s42408-018-0007-7.
Haas, J.R., Calkin, D.E., Thompson, M.P., 2013. A national approach for integrating wildfire simulation modeling into Wildland Urban Interface risk assessments within the United States. Landscape Urban Plann. 119, 44–53.
Harmon, M.E., Franklin, J.F., Swanson, F.J., Sollins, P., Gregory, S.V., Lattin, J.D., Anderson, N.H., Cline, S.P., Aumen, N.G., Sedell, J.R., Lienkaemper, G.W., Cromack, K., Cummins, J.R., Cummins, K.W., 1986. Ecology of coarse woody debris in temperate ecosystems. Adv. Ecol. Res. 15, 133–302.
Johnston, J.D., Dunn, C.J., Vernon, M.J., Bailey, J.D., Morrissette, B.A., Morici, K.E., 2018. Restoring historical forest conditions in a diverse inland Pacific Northwest landscape. Ecosphere 9 (8), e02400.
Johnston, J.D., 2017. Forest succession along a productivity gradient following fire exclusion. For. Ecol. Manage. 392, 45–57.
Jolly, W.M., Cochrane, M.A., Freeborn, P.H., Holden, Z.A., Brown, T.J., Williamson, G.J., Bowman, D.M.J.S., 2015. Climate-induced variations in global wildfire danger from 1979 to 2013. Nat. Commun. 6 (7537), 1–11.
Kennedy, R.E., Yang, Z., Cohen, W.B., 2010. Detecting trends in forest disturbance and recovery using yearly Landsat time series: 1. Landtrer – temporal segmentation algorithms. Remote Sens. Environ. 114, 2897–2910.
Larson, A.J., Belote, R.T., Cansler, C.A., Parks, S.A., Dietz, M.S., 2013. Latent resilience in ponderosa pine forest: effects of resumed frequent fire. Ecol. Appl. 23 (6), 1243–1249.
Max, T.A., Schreuder, H.T., Hazard, J.W., Oswald, D.D., Teply, J., Alegria, J. 1996. The Pacific Northwest Region vegetation and inventory monitoring system. Res. Pap. PNW-RP-493. Portland, OR: U.S. Department of Agriculture, Forest Service, Pacific Northwest Research Station, p. 22.
McDowell, N.G., Williams, A.P., Xu, C., Pockman, W.T., Dickman, T., Sevanto, S., Pangle, R., Limousin, J., Plaut, J., Mackay, D.S., Ogee, J., Domex, J.C., Allen, C.D., Fisher, R.A., Jiang, X., Muss, J., Breshears, D.D., Rauscher, S.A., Koven, C., 2015. Multi-scale predictions of massive conifer mortality due to chronic temperature rise. Nat. Clim. Change 6, 295–300.
Meddens, A.J.H., Hicke, J.A., Ferguson, C.A., 2012. Spatiotemporal patterns of observed bark beetle-caused tree mortality in British Columbia and the western United States. Ecol. Appl. 22 (7), 1876–1891.
Merschel, A.G., Spies, T.A., Heyerdahl, E.K., 2014. Mixed-conifer forests of centeral Oregon: effects of logging and fire exclusion vary with environment. Ecol. Appl. 24 (7), 1670–1688.
Miller, J.D., Thode, A.E., 2007. Quantifying burn severity in a heterogeneous landscape with a relative version of the delta normalized burn ratio (dNBR). Remote Sens. Environ. 109, 66–80.
Moritz, M.A., Batllori, E., Bradstock, R.A., Gill, A.M., Handmer, J., Hessburg, P.F., Leonard, J., McCaffrey, S., Odion, D.C., Schoennagel, T., Syphard, A.D., 2014. Learning to coexist with wildfire. Nature 515, 58–66.
Naficy, C., Sala, A., Keeling, E.G., Graham, J., DeLuca, T.H., 2010. Interactive effects of historical logging and fire exclusion on ponderosa pine forest structure in the northern Rockies. Ecol. Appl. 20, 1851–1864.
National Interagency Fire Center. 2018. https://www.nifc.gov/fireInfo/fireInfo_statistics.html. (accessed 12-01-2018).
North, M., Brought, A., Long, J., Collins, B., Bowden, P., Yasuda, D., Miller, J., Sugihara, N., 2015. Constraints on mechanized treatment significantly limit mechanical fuels reduction extent in the sierra nevada. J. Forest. 113 (1), 40–48.
O'Connor, C.D., Calkin, D.E., Thomnpson, M.P., 2017. An empirical machine learning method for predicting potential fire control locations for pre-fire planning and operational fire management. Int. J. Wildland Fire 26, 587–597.
O'Connor, C.D., Thompson, M.P., Rodriguez, Y., Silva, F., 2016. Getting ahead of the wildfire problem: quantifying and mapping management challenges and opportunities. Goesciences 6 (35), 1–18.
Ohmann, J.L., Gregory, M.J., 2002. Predictive mapping of forest composition and structure with direct gradient analysis and nearest-neighbor imputation in coastal Oregon, U.S.A. Can. J. For. Res. 32, 725–741.
Ohmann, J.L., Gregory, M.J., Roberts, H.M., Cohen, W.B., Kennedy, R.E., Yang, Z., 2012. Mapping change of older forest with nearest-neighbor imputation and Landsat timeseries. For. Ecol. Manage. 272, 13–25.
Page, W.G., Alexander, M.E., Jenkins, M.J., 2013. Wildfire's resistance to control in mountain pine beetle-attacked lodgepole pine forests. Forestry Chronicle 89 (6), 783–794.
Parks, S.A., Holsinger, L.M., Miller, C., Nelson, C.R., 2015. Wildland fire as a self-regulating mechanism: the role of previous burns and weather in limiting fire progression. Ecol. Appl. 25, 1478–1492.
Parks, S.A., Miller, C., Holsinger, L.M., Baggett, L.S., Bird, B.J., 2016. Wildland fire limits subsequent fire occurrence. Int. J. Wildland Fire 25, 182–190.
Parks, S.A., Miller, C., Nelson, C.R., Holden, Z.A., 2014. Previous fires moderate burn severity of subsequent wildland fires in two large western US wilderness areas. Ecosystems 17, 29–42.
Core Team, R., 2014. R: A language and environment for statistical computing. R Foundation for Statistical Computing, Vienna, Austria http://www.R-project.org/.
Reilly, M.J., Spies, T.A. 2015. Regional Variation in Forest Structure and Development in Oregon, Washington, and Inland Northern California, USA. Ecosphere 6:art192.
Reilly, M.J., Dunn, C.J., Meigs, G.W., Spies, T.A., Kennedy, R.E., Bailey, J.D., Briggs, K., 2017. Contemporary patterns of fire extent and severity in forests of the Pacific Northwest, USA (1985–2010). Ecosphere 8, e01695.
Reilly, M.J., Elia, M., Spies, T.A., Gregory, M.J., Sanesi, G., Lafortezza, R., 2018. Cumulative effects of wildfires on forest dynamics in the eastern Cascade Mountains, USA. Ecol. Appl. 28 (2), 291–308.
Riley, K.L., Grenfell, I.C., Finney, M.A., 2016. Mapping forest vegetation for the western United States using modified random forests imputation of FIA forest plots. Ecosphere 7 (10), e01472. https://doi.org/10.1002/ecs2.1472.
Rodriguez y Silva, F., Molina Martinez, J.R., Gonzalez-Caban, A., 2014. A methodology for determing operational priorities for prevention and suppression of wildland fires. Int. J. Wildland Fire 23, 544–554.
Scott, Joe H., Thompson, Matthew P., Calkin, David E., 2013. A wildfire risk assessment framework for land and resource management. In: Gen. Tech. Rep. RMRS-GTR-315. U.S. Department of Agriculture, Forest Service, Rocky Mountain Research Station, pp. 83.
Stephens, S.L., Burrows, N., Buyantuyev, A., Gray, R.W., Keane, R.E., Kubian, R., Liu, S., Seijo, F., Shu, L., Tolhurst, K.G., van Wagtendonk, J.W., 2014. Temperate and boreal forest mega-fires: characteristics and challenges. Front. Ecol. Environ. 12, 115–122.
Stevens, J.T., Collins, B.M., Miller, J.D., North, M.P., Stephens, S.L., 2017. Changing spatial patterns of stand-replacing fire in California conifer forests. For. Ecol. Manage. 406, 29–36.
Stevens-Rumann, C.S., Kemp, K.B., Higuera, P.E., Harvey, B.J., Rother, M.T., Donato, D.C., Morgan, P., Veblen, T.T., 2018. Evidence for declining forest resilience to wildfires under climate change. Ecol. Lett. 21 (2), 243–252.
Swanson, M.E., Franklin, J.F., Beschta, R.L., Crisafulli, C.M., DellaSala, D.A., Hutto, R.L., Lindenmayer, D.B., Swanson, F.J., 2010. The forgotten stage of forest succession: early-successional ecosystems on forest sites. Front. Ecol. Evniron. 9 (2), 1–10.
Ter Braak, C.J., 1986. Canonical correspondence analysis: a new eigenvector technique for multivarite direct gradient analysis. Ecology 67 (5), 1167–1179.
Thomas, J.W., Anderson, R.G., Maser, C., Bull, E.L., 1979. Snags. In: Thomas, J.W. (Ed.), Wildlife Habitats in Managed Forests: The Blue Mountains of Oregon and Washington. USDA Forest Service Agriculture Handbook No. 553, pp. 77–95.
Thompson, M.P., Calkin, D.E., 2011. Uncertainty and risk in wildand fire managemetn: a review. 2011. J. Environ. Manage. 92, 1895–1909.
Thompson, M.P., Dunn, C.J., Calkin, D.E., 2015. Wildfires: Systemic changes required. Science 350 (6263), 920.
Thompson, M.P., Freeborn, P., Rieck, J.D., Calkin, D.E., Gilbertson-Day, J.W., Chocrane, M.A., Hand, M.S., 2016a. Quantifying the influence of previously burned areas on suppression effectiveness and avoided exposure: a case study of the Las Conchas Fire. Int. J. Wildland Fire 25, 167–181.
Thompson, M.P., MacGregor, D.G., Calkin, D.E., 2016b. Risk management: core principles and practices, and their relevance to wildland fire. In: Gen. Tech. Rep. RMRS-GTR-350. Fort Collins, CO: U.S. Department of Agriculture, Forest Service, Rocky Mountain Research Station, pp. 29.
Thompson, M.P., MacGregor, D.G., Dunn, C.J., Calkin, D.E., Phipps, J., 2018. Rethinking the wildland fire management system. J. Forest. 116 (4), 382–390.
Tinker, D.B., Knight, D.H., 2000. Coarse woody debris following fire and logging in Wyoming lodgepole pine forests. Ecosystems 3, 472–483.
VanDerWal, J., Lorena Falconi, L., Januchowski, S., Shoo, L., Storlie, C. 2014. SDMTools: Species Distribution Modelling Tools: Tools for Processing Data Associated with Species Distribution Modelling exercises. R package version 1.1-221. http://CRAN.R-project.org/package=SDMTools.
Zald, H.S.J., Dunn, C.J., 2018. Sever fire weather and intensive forest management increase fire severity in a multi-ownership landscape. Ecol. Appl. 28 (4), 1068–1080.